Adaptive Extended Kalman Filter for Indoor/Outdoor Localization using a 802.15.4a Wireless Network

A. Benini A. Mancini E. Frontoni P. Zingaretti S. Longhi
Dipartimento di Ingegneria Informatica Gestionale e dell'Automazione (DIIGA)
Università Politecnica delle Marche, Ancona, Italy

***Abstract*— Indoor and outdoor localization of mobile robots using wireless technologies is very attractive in many applications as cooperative robotics. Wireless networks can be successfully used not only for communication among heterogeneous vehicles (e.g., ground, aerial) but also for localization. This paper introduces an approach for the indoor/outdoor localization of a mobile robot using IEEE 802.15.4a devices with ranging capability based on Symmetrical Double-Sided Two Way Ranging (SDS-TWR). This technique tries to overtake the limitations of the classical one Received Signal Strength Indication (RSSI) (e.g., Wi-fi mapping) that does not ensure good performance especially in structured environments. The set of these devices allows to create a Wireless Sensor Network (WSN) that is suitable for cooperative tasks where the data link is fundamental to share data and support the relative localization. In this paper an Adaptive Extended Kalman Filter (EKF) is introduced as a possible technique to improve the localization in both outdoor and indoor environments also in real time due to a reduced computational complexity. The proposed approach allows to model the bias of ranging data considering also the faults in the measurements. The obtained results put in evidence the necessity of further ranging data to obtain centimetric accuracy and precision of localization that actually is rated to 1m.**

***Index Terms*— Localization, Ranging, IEEE 802.15.4a, WSN**

I. Introduction

INDOOR and outdoor location of mobile robots using wireless technologies is very attractive in many application. Wireless networks can be successfully used not only for communication between devices but also for localization. IEEE 802.15.4a specifies two additional physical layers (PHYs): a PHY using ultra-wideband (UWB) and a PHY using chirp spread spectrum (CSS) both with a precision time-based ranging capability [1], [2], [3], [4], [5], [6].

The UWB PHY is operating in three frequency bands: below 1 GHz, between 3 and 5 GHz, and between 6 and 10 GHz. The UWB physical layer channels have large bandwidth and provide high ranging accuracy, up to 1 meter. The main advantages of UWB technology are high data transfer, low power consumption, high spatial capacity of wireless data transmission and sophisticated usage of radio frequencies. UWB technology is based on sending and receiving carrierless radio impulses using extremely accurate timing. UWB can be used for example in such applications where high bandwidth signals must be transmitted between devices.

The CSS PHY is operating in 2.4 GHz ISM band. The chirp solution does not support ranging, but the first 802.15.4a CSS chip (nanoLOC) developed by Nanotron has the ranging as additional (proprietary) function. It offers a unique solution for devices moving at high speeds because of its immunity to Doppler Effect and provides communicating at longer ranges.

The main problem of time-based range measurement consists in multipath and non-line-of-sight (NLOS) measurements. Since for time-based ranging measurement the line-of-sight (LOS) between sensors are needed, indoor and outdoor measurements can be affected by bias due to presence of obstacles, metallic surfaces and/or electromagnetic fields.

This paper studies the indoor/outdoor localization of a mobile robot using the nanoLoc WSN system in conjunction with a Extended Kalman Filter (EKF) in order to improve the position accuracy considering also the bias.

The nanoLOC Development Kit is a complete, easy to use set of tools for evaluating, prototyping and developing applications based on Nanotron's nanoLOC TRX Transceiver. nanoLOC is a highly integrated mixed signal chip utilizing Nanotron unique Chirp Spread Spectrum (CSS) technology. It provides built-in ranging in the globally available 2.4 GHz ISM band [7].

A review of existing ranging techniques is provided in [8]. The most important methodologies for ranging calculation are listed below:

- Angle of Arrival (AoA)
- Time of Arrival (ToA)
- Time Difference of Arrival (TDoA)
- Received Signal Strength Indication (RSSI)
- Symmetrical Double Sided Two Way Ranging (SDS-TWR)

The Angle of Arrival, or AoA, is a method for determining the direction of propagation of an RF signal received from a tag to an anchor. Using directional antennas, an estimate of the direction of the tag can be obtained. The Angle of Arrival is determined by measuring the angle between a line that runs from the anchor to the tag and a line from the reader and a predefined direction, for instance the position of a known point. When the signal to noise ratio is relatively high, the angle of arrival of the strongest signal can be estimated with a very simple methods. The differences in the arrival times of the wideband signal received by spatially separated sensors can be estimated using the polarity coincidence correlation. These time differences, (for example time delays), determine the angle of arrival. In [9] the effects of quantization of the time delays are studied. It is found out that this simple

method gives comparable performance to the conventional, direct correlation based methods in the case of a relatively high signal to noise ratio.

The Time of Arrival, or ToA, is a method based on the measurement of the propagation delay of the radio signal between a transmitter (tag) and one or more receivers (anchors). The accuracy of measuring the distance using this method is sensitive to the bandwidth of the system and the multipath condition between the wireless terminal and the access point. In general, as the bandwidth increases beyond a certain value, it is expected that the measured TOA error approaches zero. However, for the undetected direct path (UDP) conditions, the system exhibits substantially high distance measurement errors that cannot be eliminated with the increase in the bandwidth of the system. In [10], an analysis of the behaviour of super-resolution and traditional TOA estimation algorithms in line-of-sight (LOS), non- LOS, and UDP conditions in indoor areas is presented.

The Time Difference of Arrival (TDOA) method is slightly different from ToA. Systems using the TDOA method measures the difference in transmission time between the signals received from each transmitter to a tag.

The RSSI (Received Signal Strength Indication) allows the location of a device based on the strength of signals sent from the anchors to the device that is to be localized [11]. To determine the location of the tag by means of this technique, at least three anchors are needed. In a location system based on RSSI, the distance between the tag and one of the anchors is based on the difference between the power of the signal transmitted from the anchor and the one received by the tag. To be effective, RSSI requires a dense deployment of Access Points, which increase considerably to the cost of the system. However, the key problem related to RSSI- based systems is that an adequate underlying path-loss model must be found for both non-line-of-sight and non-stationary environments. Consequently, in practice, estimated distances are somewhat unreliable. In [12], the effects of different frequencies on RSSI measurements and a methods to increasing the distance measurement accuracy is provided.

The operating principle of the SDS-TWR technique is similar to the principle on which the TOF is based: it avoids the need to synchronize the clocks of the nodes used in ranging measurements. The SDS-TWR bases its operation on the basis of two delays that naturally characterize the transmission of signals in the ether propagation:

- Propagation delay of the signal between two devices
- Time needed for signal processing inside devices

This technique is called Symmetrical Double-Sided Two Way Ranging, because:

- It is symmetric: the measurement from the tag T and the anchor A is a mirror-image of the measurement made from anchor A to the tag T (TAT to ATA);
- It is double-sided: only two devices (Tag and Anchor) are needed for ranging;
- It is two-way ranging because SDS-TWR works with sending and receiving of ACK packets and information packets;

During the SDS-TWR measurements, one node (Tag) sends a packet to a second node (Anchor) and starts the time counting. The time measurement on second node starts from the reception of the packet until the propagation of packet back to the first node. When the first node receives the acknowledgement from the second one, it stops the time counting and store the value in its memory.
The acknowledgement sent back to the first node includes in its header two delay values - the Signal Propagation Delay and the Processing Delay. After this, the entire process is repeated from second node to the first. At the end of this procedure, two range values are determined and an average of the two can be used to achieve a fairly accurate distance measurement between these two nodes (Fig. 1). SDS-TWR does not require any kind of time synchronization between the transmitter and the receiver; instead it only depends on time-of-flight between two devices in order to estimate the range. As reported in [13], SDS-TWR technology demonstrates a superiority over other localization methods in that it removes the time synchronization between devices, which is a quite demanding requirement.

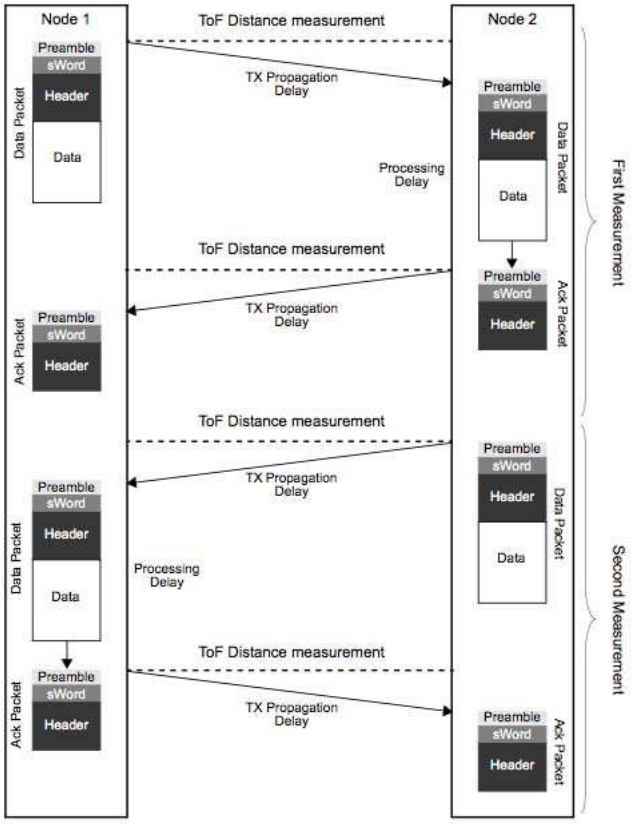

Fig. 1. Simmetric Double Sided Two Way Ranging Technique

II. The NanoLoc Localization System

Nanotron Technologies has developed a WSN system that allows the development of RTLS applications. The distance between two wireless nodes is determined using the Simmetric Double Sided Two Way Ranging (SDS-TWR)

technique. Both, the wireless communication technology and SDS-TWR technology are integrated into a single chip, the nanoLOC TRX Transceiver [14]. The transceiver operates on S.4 GHz ISM band and supports not only location-aware applications but also robust wireless communication. Wireless communication is based on Nanotron Chirp Spread Spectrum (CSS) according to IEEE 802.15.4a wireless standard. Data rates are selectable from 125kbit/s to 2Mbit/s.

III. The Extended Kalman Filter

The Kalman Filter is suitable for the estimation of x and y coordinates of a mobile device (tag) on the basis of ranging measurements made between the tag and at least three known points (anchors). Let denote with $(a_{x,i}, a_{y,i})$ $(i = 1, ..., n)$ the x and y coordinates of the anchors and with $\mathbf{T} = (t_x, t_y)^T$ the unknown tag coordinates. The distance between an anchor and the tag is calculated in the following way:

$$d_i = \sqrt{(t_x - a_{x,i})^2 + (t_y - a_{y,i})^2} \tag{1}$$

The tag position can be obtained by trilateration as follows:

$$\mathbf{H} \cdot \begin{pmatrix} t_x \\ t_y \end{pmatrix} = \mathbf{z} \tag{2}$$

where

$$\mathbf{H} = \begin{pmatrix} 2 \cdot a_{x,1} - 2 \cdot a_{x,2} & 2 \cdot a_{y,1} - 2 \cdot a_{y,2} \\ \vdots & \vdots \\ 2 \cdot a_{x,1} - 2 \cdot a_{x,n} & 2 \cdot a_{y,1} - 2 \cdot a_{y,n} \end{pmatrix} \tag{3}$$

and

$$\mathbf{z} = \begin{pmatrix} d_2^2 - d_1^2 + a_{x,1}^2 - a_{x,2}^2 + a_{y,1}^2 - a_{y,2}^2 \\ \vdots \\ d_n^2 - d_1^2 + a_{x,1}^2 - a_{x,n}^2 + a_{y,1}^2 - a_{y,n}^2 \end{pmatrix} \tag{4}$$

An estimation of $\mathbf{T}$ can be obtained using the method of least squares:

$$\begin{pmatrix} \hat{t}_x \\ \hat{t}_y \end{pmatrix} = (\mathbf{H}^T \mathbf{H})^{-1} \mathbf{H}^T \cdot \mathbf{z} \tag{5}$$

In the extended Kalman filter (EKF), the state transition and observation models need not be linear functions of the state but may instead be differentiable functions:

$$\begin{aligned} \tilde{\mathbf{x}}_{k+1} &= \mathbf{f}(\hat{\mathbf{x}}_k, \mathbf{u}_k, \mathbf{w}_k), \\ \tilde{\mathbf{y}}_{k+1} &= \mathbf{h}(\tilde{\mathbf{x}}_{k+1}, \mathbf{v}_{k+1}) \end{aligned} \tag{6}$$

where $\tilde{\mathbf{x}}_k$ and $\tilde{\mathbf{y}}_k$ denote respectively the approximated *a priori* state and observation and $\hat{\mathbf{x}}_k$ the *a posteriori* estimate of the previous step. The state vector contains the predicted tag coordinate as expressed in the following equation:

$$\mathbf{x}_k = \begin{pmatrix} t_{kx} \\ t_{ky} \end{pmatrix} \tag{7}$$

Referring to the state estimation, the process is characterized by the statistical variables $\mathbf{w}_k$ and $\mathbf{v}_k$ that represent respectively the process noise and measurement noise. $\mathbf{W}_k$ and $\mathbf{v}_k$ are supposed to be independent, white and normal probably distributed with given covariances matrix $\mathbf{Q}_k$ and $\mathbf{R}_k$. The observation vector $\boldsymbol{y}_k$ represents ranging measurements made between tag and anchors, and defines the entry parameter of the filter. Because in the analyzed system the predictor equation contains a linear relationship, the process function $\boldsymbol{f}$ can be expressed as a linear function:

$$\mathbf{x}_{k+1} = \mathbf{A}\mathbf{x}_k + \mathbf{B}\mathbf{u}_k + \mathbf{w}_k \tag{8}$$

where the transition matrix $\boldsymbol{A}$ and $\boldsymbol{B}$ are defined as follows:

$$\mathbf{A} = \begin{pmatrix} 1 & 0 & -u_t \sin\theta_k \\ 0 & 1 & u_t \cos\theta_k \\ 0 & 0 & 1 \end{pmatrix}, \quad \mathbf{B} = \begin{pmatrix} \cos\theta_k & 0 \\ \sin\theta_k & 0 \\ 0 & 1 \end{pmatrix}. \tag{9}$$

and T is the time sample. The input control vector contains the linear (u_t) and angular (u_a) speed of the robot:

$$\mathbf{u}_k = \begin{pmatrix} u_t \\ u_a \end{pmatrix} \tag{10}$$

The equation $\tilde{\mathbf{y}}_{k+1} = \mathbf{h}(\tilde{\mathbf{x}}_{k+1}, \mathbf{v}_{k+1})$ is calculated in the following way:

$$\begin{pmatrix} \hat{r}_1 \\ \vdots \\ \hat{r}_n \end{pmatrix} = \begin{pmatrix} \sqrt{(\tilde{t}_x - a_{x,1})^2 + (\tilde{t}_y - a_{y,1})^2} \\ \vdots \\ \sqrt{(\tilde{t}_x - a_{x,n})^2 + (\tilde{t}_y - a_{y,n})^2} \end{pmatrix} + \mathbf{v}_{k+1} \tag{11}$$

and the related Jacobian matrix $\boldsymbol{C}_{k+1} = \dfrac{\partial \boldsymbol{h}}{\partial \boldsymbol{x}}(\tilde{x}_k, 0)$ is given as:

$$\boldsymbol{C}_{k+1} = \begin{pmatrix} \dfrac{\partial \hat{r}_1}{\partial \tilde{t}_x} & \dfrac{\partial \hat{r}_1}{\partial \tilde{t}_y} \\ \vdots & \vdots \\ \dfrac{\partial \hat{r}_n}{\partial \tilde{t}_x} & \dfrac{\partial \hat{r}_n}{\partial \tilde{t}_y} \end{pmatrix} \tag{12}$$

where

$$\begin{aligned} \frac{\partial \hat{r}_i}{\partial \tilde{t}_x} &= \frac{\tilde{t}_x - a_{x,i}}{\sqrt{(\tilde{t}_x - a_{x,1})^2 + (\tilde{t}_y - a_{y,1})^2}}, \\ \frac{\partial \hat{r}_i}{\partial \tilde{t}_y} &= \frac{\tilde{t}_y - a_{y,i}}{\sqrt{(\tilde{t}_x - a_{x,1})^2 + (\tilde{t}_y - a_{y,1})^2}} \end{aligned} \tag{13}$$

A. Detection of faulty range measurements

The measures provided by Nanotron sensors are accompanied with flags that indicate whether the measure was made correctly or not. Specifically, if the ranging r_i is done correctly, the corresponding flag variable is set to 15. Otherwise, the flag variable assumes a different value depending on the type of failure occurred. If a fault on a measurement is detected, the corresponding element of the measurement covariance matrix $\boldsymbol{R}$ is increased:

$$\boldsymbol{R} = \begin{pmatrix} \sigma_{r,1}^2 & 0 & \cdots & 0 \\ 0 & \sigma_{r,2}^2 & \cdots & 0 \\ \vdots & \vdots & \ddots & \vdots \\ 0 & 0 & \cdots & \sigma_{r,n}^2 \end{pmatrix} \tag{14}$$

where $\sigma^2_{r,i}$ can be identified by experiments. In [15], [16], after a series of tests, authors set $\sigma^2_{r,1} = 0.1328m^2$. Depending of presence of a fault, the $i-th$ element of $\boldsymbol{R}$ matrix is set in the following way:

$$\sigma^2_{r,i} = \begin{cases} \beta\sigma^2_{r,i} : \text{with fault} \\ \sigma^2_{r,i} : \text{without fault} \end{cases} \quad (15)$$

where β is chosen by experiments to give a good localization performance; in the following tests, β is set to 10^5.

B. The Extended Kalman Filter with bias modelling

The model discussed in the previous paragraphs is based on the assumption that the measured distances contain only noise. However, range measurements made with CSS sensor non only have noise but also a non-zero average error. This non-zero average error can be treated as a bias. In this case, the measured distance, at time k, referring to anchor i can be modelled more accurately in the following way:

$$\overline{y}_{ki} = d_{ki} + v_{ki} + b_{ki} \quad (16)$$

where $\overline{y}_{ki}$ denotes the biased measure and b_{ki} the bias related to anchor i at time k. The bias vector is difficult to manage because it is not possible to measure it. A strategy could be to estimate the bias vector by subtracting the estimated bias vector from the measured distance vector [17]. But in more cases this is not possible because the bias vector depends on more factor as multipath or presence of moving obstacles. To model the bias change, we introduce a scaling factor s_k which satisfies the following relationship:

$$\mathbf{d}_{ki} + \mathbf{b}_{ki} \approx (1 + s_k)\mathbf{d}_{ki} \quad (17)$$

By using 17, we can derive a new formulation of the measurement model:

$$\overline{y}_{ki} = (1 + s_k)d_{ki} + v_{ki} \quad (18)$$

We assume that the bias hardly changes during an iteration; thus, the scaling factor is expressed as $s_{k+1} = s_k$ and the process noise of the scaling factor as w_{rk}. Now we can extend the EKF by adding a new state variable describing the bias that affects range measurements:

$$\begin{aligned} \tilde{\overline{\mathbf{x}}}_{k+1} &= \mathbf{f}(\hat{\overline{\mathbf{x}}}_k, \overline{\mathbf{u}}_k, \overline{\mathbf{w}}_k), \\ \tilde{\overline{\mathbf{y}}}_{k+1} &= \mathbf{h}(\tilde{\overline{\mathbf{x}}}_{k+1}, \overline{\mathbf{v}}_{k+1}) \end{aligned} \quad (19)$$

where

$$\overline{\mathbf{x}}_k = \begin{pmatrix} \mathbf{x}_k \\ s_k \end{pmatrix} \quad (20)$$

$$\overline{\mathbf{u}}_k = \begin{pmatrix} \mathbf{u}_k \\ 0 \end{pmatrix} \quad (21)$$

$$\overline{\mathbf{w}}_k = \begin{pmatrix} \mathbf{w}_k \\ w_{rk} \end{pmatrix} \quad (22)$$

IV. Experimental Results

In this sections the localization experiments in two different environments are presented. The first environment is critical due to the presence of walls with metallic surfaces that make not possible the use of GPS. The second test allows to evaluate the performance in terms of accuracy and precision considering the GPS trace as ground truth.

A. Configuration of the experiments

The architecture of the mobile robotic platform (see Fig. 2) is aligned with a typical outdoor SLAM mission. The selected mobile robotic platform is the Pioneer P3-AT produced by the MobileRobots Inc. This platform is suitable for outdoor environments and can hold a payload of 12kg.

The instrumentation payload is formed by:

- Differential Global Positioning System (DGPS) Topcon GR3 receiver;
- Inertial Sensor (Microstrain 3DM-GX1);
- Nanotron tag.

The DGPS receiver is coupled with a master station (same kind of receiver) to increase the accuracy and the precision of positioning data; the antenna is mounted at 0.5m over ground to avoid dangerous reflections and/or signal attenuation due to the presence of obstacles. In kinematic mode the obtained accuracy and precision was $< 2cm$. A Real Time Operating System (RTOS) provides access to robot by means of a set of software tools (e.g., ARIA and Carmen) included in the Robobuntu Linux distro [18], [19].

Fig. 2. Robotic platform

B. Experimental results in Environment $n°1$

In this subsection the localization results in a indoor environment are presented. The reason of this choice is for the performances evaluations in presence of multipath.

We assigned 2-D Cartesian coordinates of anchors with the following values:

$$\begin{aligned}\mathbf{A}_1 &= [11.90 \quad 0.15]^T \\ \mathbf{A}_2 &= [21.00 \quad 2.30]^T \\ \mathbf{A}_3 &= [30.90 \quad 0.15]^T \\ \mathbf{A}_4 &= [47.54 \quad 2.30]^T\end{aligned} \tag{23}$$

The unit of these coordinates was meter. The following figure (Fig. 3) shows the indoor environment (environment $n^\circ 1$):

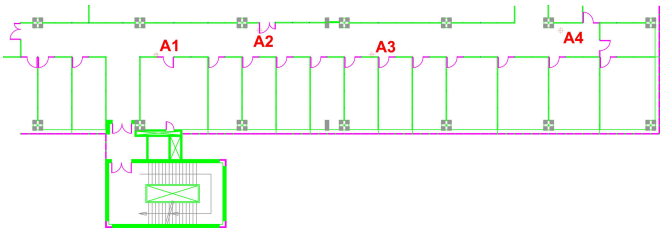

Fig. 3. Map of the environment $n^\circ 1$

The maximum speed of the robot is set to $0.8m/s$. While the mobile robot moves along the path, the CSS tag node attached to the robot measures ranging from the four anchors. First the tag measures the distance form anchor 1 (A1), after the distances from anchors 2 (A2), and so on. Because the time required to obtain the four ranging measurements is fast ($0.05s$) compared to the speed of the robot, we assume that the four distances were measured at the same time.

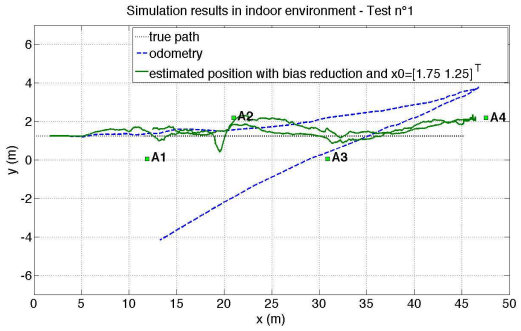

Fig. 4. Test $n^\circ 1$ in environment $n^\circ 1$

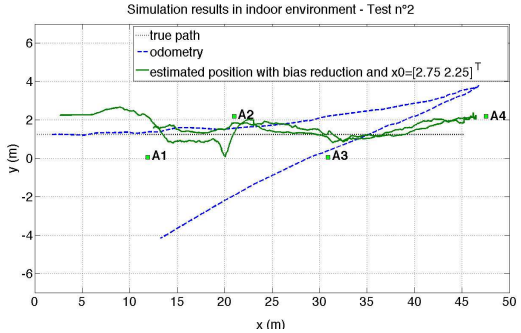

Fig. 5. Test $n^\circ 2$ in environment $n^\circ 1$

In Test n.1 the true position of the robot at the beginning of the test is $[1.70 \quad 1.25]^T m$, while in test n.2 is $[2.75 \quad 2.25]^T m$.

The obtained results (see Figures 4 and 5) show that the filter allows to obtain better result in terms of localization due to the estimation of bias; its amplitude is 1m circa. The filter is also able to track the position of robot considering a high uncertainty in the initial position (green line in Fig.5) adjusting the error covariance matrix P at time 0. In this case the mean error is approximately 1m.

C. Experimental results in Environment $n^\circ 2$

In this second series of test we chose an outdoor environment without obstacles. The reason of this choice is for the performances evaluations in an open space. The 2-D Cartesian coordinates of anchors have the following values:

$$\begin{aligned}\mathbf{A}_1 &= [0 \quad 0]^T \\ \mathbf{A}_2 &= [17.1 \quad 36.5]^T \\ \mathbf{A}_3 &= [-12.0 \quad 50.3]^T \\ \mathbf{A}_4 &= [-29.4 \quad 13.8]^T\end{aligned} \tag{24}$$

The unit of these coordinates was meter.

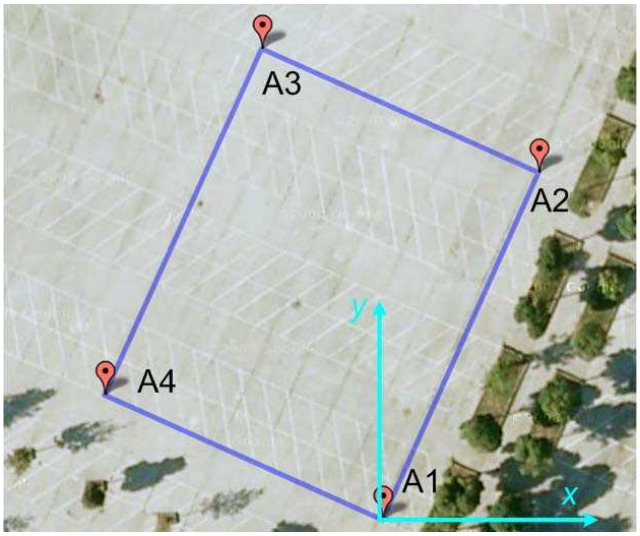

Fig. 6. Map of the environment $n^\circ 2$

In Fig. 7 the obtained results are presented. The green dashed lines represent the estimation of path using the odometric information obtained by on board encoders integrated with a MEMS gyro and Nanotron Sensors. The blue one represent the true path calculated with differential GPS (DGPS).

The gyro is necessary to estimate the rotation speed of robot due to high friction of wheels with the rough terrain. The EKF filter allows to reduce the localization error if compared with the standard dead reckoning. The blue lines represent the ground truth obtained by the GPS with differential corrections.

The EKF is also able to manage the loss of anchor due to a temporary / continuous fault (e.g., anchor too far,

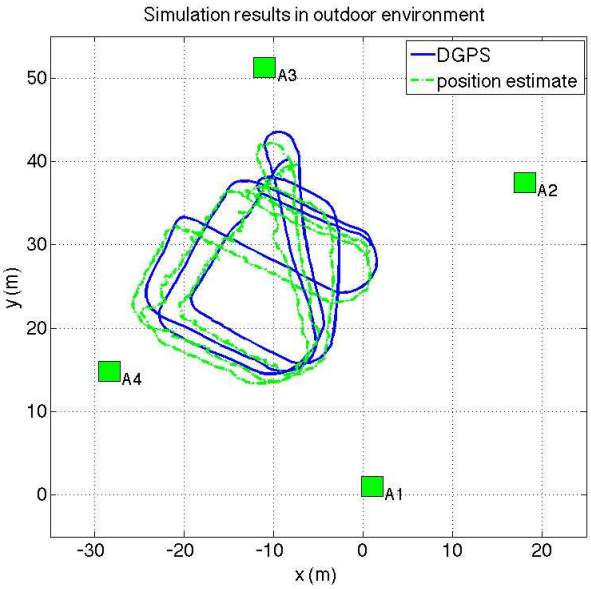

Fig. 7. Test $n°1$ in environment $n°2$

low battery, high occlusion). Considering the total network traffic the 80% of packets contains useful ranging data. The remaining 20% contains invalid data (e.g., out of range) that are managed by the EKF.

V. Conclusion and Future Works

In this paper a Extended Kalman filter for indoor/outdoor localization using a 802.15.4a Wireless Network was presented considering also the bias. The paper present two different approaches based on the Kalman approach to estimate the position of robot using ranging data from the Wireless Network. The algorithms are able to manage measurement faults isolating the corrupted data without shutting down the localization approach. The obtained results reinforces the necessity of integrate additional sensors to obtain better results in terms of accuracy and precision. In case of indoor environments the integration of Laser Range Finder or camera (with SIFT/SURF) extractor could significantly improve the overall performance.

Future works will be steered to extend the set of sensors integrating visual information based on SIFT/SURF [20] and to evaluate this technology also for small size unmanned aerial systems as quad-rotors that are suitable for indoor environments.

Acknowledgments

This work is developed in the context of ARTEMIS-JU EU Project R3-COP. In particular the authors would like to thank Mauro Montanari and Riccardo Minutolo (Thales Italia S.p.A) for their support.

References

[1] Z. Sahinoglu and S. Gezici. Ranging in the ieee 802.15.4a standard. In *IEEE Annual Wireless and Microwave Technology Conference, 2006. WAMICON '06.*, pages 1 –5, dec. 2006.

[2] Hyeonwoo Cho and Sang Woo Kim. Mobile robot localization using biased chirp-spread-spectrum ranging. *IEEE Transactions on Industrial Electronics*, 57(8):2826 –2835, aug. 2010.

[3] C. Rohrig, D. Hes, C. Kirsch, and F. Kunemund. Localization of an omnidirectional transport robot using ieee 802.15.4a ranging and laser range finder. In *Proceedings of the 2010 IEEE/RSJ International Conference on Intelligent Robots and Systems (IROS 2010)*, pages 3798–3803, October 2010.

[4] A. Sikora and V.F. Groza. Fields tests for ranging and localization with time-of-flight-measurements using chirp spread spectrum rf-devices. In *IEEE Instrumentation and Measurement Technology Conference Proceedings, 2007. IMTC 2007.*, pages 1 –6, may 2007.

[5] Jae-Eon Kim, Jihoon Kang, Daeyoung Kim, Younghwoon Ko, and Jungsik Kim. Ieee 802.15.4a css-based localization system for wireless sensor networks. In *IEEE Internatonal Conference on Mobile Adhoc and Sensor Systems, 2007. MASS 2007.*, pages 1 –3, oct. 2007.

[6] S. Krishnan, P. Sharma, Zhang Guoping, and Ong Hwee Woon. A uwb based localization system for indoor robot navigation. In *IEEE International Conference on Ultra-Wideband, 2007. ICUWB 2007.*, pages 77 –82, sept. 2007.

[7] Nanotron technologies gmbh - `http://www.nanotron.com`.

[8] A.H. Sayed, A. Tarighat, and N. Khajehnouri. Network-based wireless location: challenges faced in developing techniques for accurate wireless location information. *Signal Processing Magazine, IEEE*, 22(4):24 – 40, july 2005.

[9] Jari Yli-hietanen, Kari Kalliojarvi, and Jaakko Astola. Low-complexity angle of arrival estimation of wideband signals using small arrays. In *In Proceedings of the 8th IEEE Signal Processing Workshop on Statistical Signal and Array Signal Processing*, pages 109–112, 1996.

[10] N. Alsindi, Xinrong Li, and K. Pahlavan. Analysis of time of arrival estimation using wideband measurements of indoor radio propagations. *IEEE Transactions on Instrumentation and Measurement*, 56(5):1537 –1545, oct. 2007.

[11] A.S. Paul and E.A. Wan. Rssi-based indoor localization and tracking using sigma-point kalman smoothers. *IEEE Journal of Selected Topics in Signal Processing*, 3(5):860 –873, oct. 2009.

[12] Osman Ceylan, K. Firat Taraktas, and H. Bulent Yagci. Enhancing rssi technologies in wireless sensor networks by using different frequencies. In *Proceedings of the 2010 International Conference on Broadband, Wireless Computing, Communication and Applications*, BWCCA '10, pages 369–372, Washington, DC, USA, 2010. IEEE Computer Society.

[13] Hyo-Sung Ahn, Hwan Hur, and Wan-Sik Choi. One-way ranging technique for css-based indoor localization. In *Industrial Informatics, 2008. INDIN 2008. 6th IEEE International Conference on*, pages 1513 –1518, july 2008.

[14] "nanoloc trx transceiver (na5tr1)", nanotron technologies gmbh, berlin, germany, datasheet na-06-0230-0388-2.00, apr. 2008.

[15] C. Rohrig and M. Muller. Indoor location tracking in non-line-of-sight environments using a ieee 802.15.4a wireless network. In *IEEE/RSJ International Conference on Intelligent Robots and Systems, 2009. IROS 2009*, pages 552 –557, oct. 2009.

[16] S. Spieker and C. Rohrig. Localization of pallets in warehouses using wireless sensor networks. In *16th Mediterranean Conference on Control and Automation, 2008*, pages 1833 –1838, june 2008.

[17] F. Capezio, A. Sgorbissa, and R. Zaccaria. An augmented state vector approach to gps-based localization. In *Intelligent Robots and Systems, 2007. IROS 2007. IEEE/RSJ International Conference on*, pages 2480 –2485, 29 2007-nov. 2 2007.

[18] A. Mancini, E. Frontoni, A. Ascani, and P. Zingaretti. Robobuntu: A linux distribution for mobile robotics. pages 2544 –2549, may. 2009.

[19] robobuntu linux distribution. `http://www.robobuntu.diiga.univpm.it`.

[20] Andrea Ascani, Emanuele Frontoni, Adriano Mancini, and Primo Zingaretti. Feature group matching for appearance-based localization. In *IROS*, pages 3933–3938, 2008.